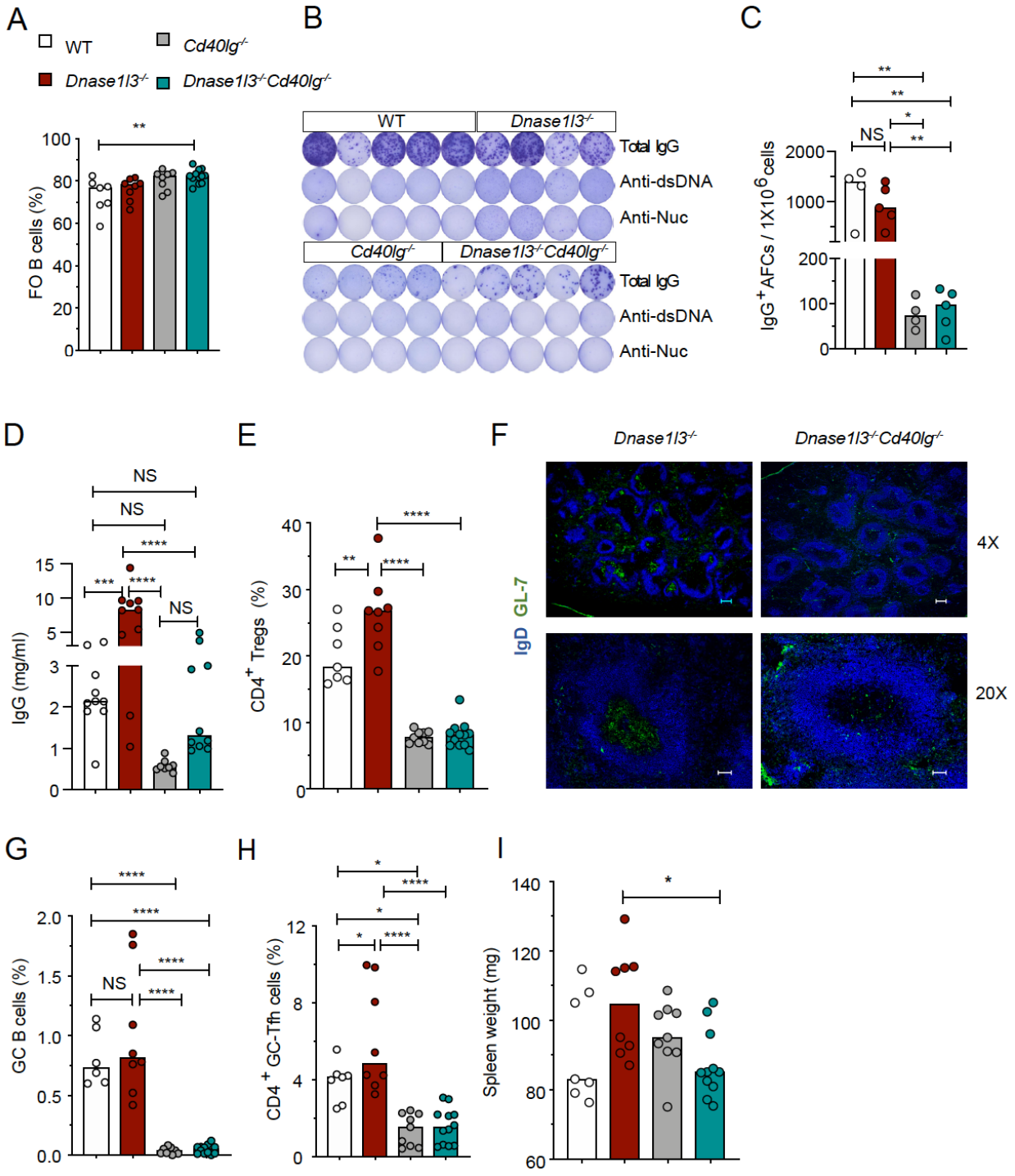

Figure S1. *Dnase1l3*$^{-/-}$*Cd40lg*$^{-/-}$ mice do not develop autoimmunity, Related to Figure 1.
Mice: *Dnase1l3*$^{-/-}$ (red symbols), CD40L (*Cd40lg*$^{-/-}$, grey symbols), *Dnase1l3*$^{-/-}$*Cd40lg*$^{-/-}$mice (green symbols) or wild-type controls (WT, open symbols). In all panels, symbols represent individual mice and bars indicate median, wherever applicable.
(A) Frequency of CD23^{+}CD21^{-} follicular (FO) B cells among total CD19^{+}B220^{+} B cells from 12-mo-old mice as determined by flow cytometry.
(B) ELISpot image showing comparative analysis of ImmunoSpots of anti-IgG, anti-dsDNA, and anti-nucleosome antibody-forming cells (AFCs), in the spleen of 12-mo-old mice.

(C) Total number of anti-IgG antibody-forming cells (AFCs) in the spleen of 12-mo-old mice as determined by ELISpot (AFC per 10^6 total cells).
(D) Total IgG in the serum of 12-mo old mice as measured by ELISA.
(E) Frequency of $CD25^+FOXP3^+$ T-regulatory cells among $CD4^+$ T cells of 12-mo-old mice as determined by flow cytometry.
(F) Representative immunofluorescence images of spleen sections from 12-mo-old-mice of indicated strains stained for IgD^+ naïve follicular B cells (blue) and GL-7^+ GC B cells (green). Upper panels scale bar 100 μm, lower panels 30 μm.
(G) Fractions of $CD38^-$ GL-7^+ GC B cells among total $CD19^+B220^+$ splenic B cells from 12-mo-old mice, as determined by flow cytometry.
(H) Fractions of $CXCR5^{hi}PD\text{-}1^{hi}$ GC-Tfh population among $CD4^+$ splenic T cells from 12-mo-old mice, as determined by flow cytometry.
(I) Spleen weight of mice at 12-months of age.
One-way ANOVA followed by the Tukey multiple-comparison test was used for statistical analysis of more than two groups. Statistical significance: * $p \leq 0.05$, ** $p \leq 0.01$, and **** $p \leq 0.0001$.

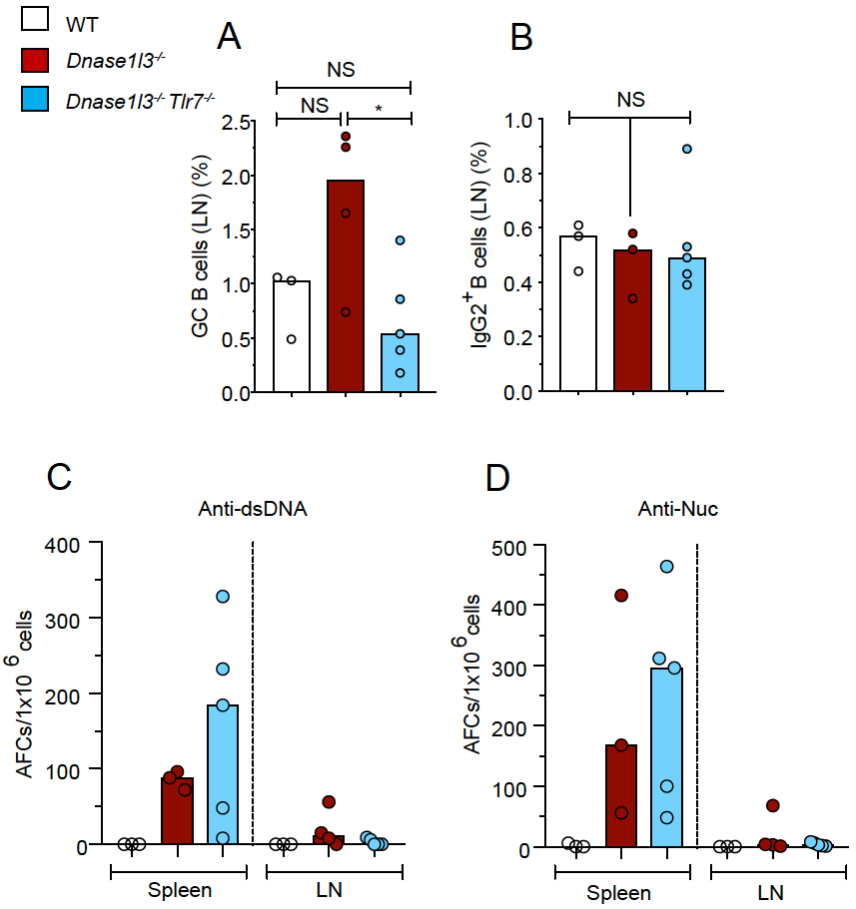

Figure S2. Anti-dsDNA and anti-Nuc AFCs in *Dnase1l3*$^{-/-}$ and *Dnase1l3*$^{-/-}$*Tlr7*$^{-/-}$ mice develop in the spleen and not in LNs, Related to Figure 2.

Mice: *Dnase1l3*$^{-/-}$ were examined along with *Dnase1l3*$^{-/-}$*Tlr7*$^{-/-}$ mice (blue symbols) and wild-type controls (WT, open symbols). In panels A-D, symbols represent individual mice and bars indicate median.

(A and B) Fraction of CD38^{-}GL-7^{+} GC B cells (A) and IgD^{-}IgM^{-}IgG2a/2b^{+} (switched) cells among CD19^{+}B220^{+} B cells from inguinal and mesenteric lymph nodes (LNs) of 6-8-mo-old mice as determined by flow cytometry.

(C and D) Total number of anti-dsDNA (C) and anti-nucleosome (D) antibody forming cells (AFCs) in the spleen and corresponding inguinal/ mesenteric lymph nodes (LN) of 6-8-mo-old mice determined by ELISpot assay.

One-way ANOVA followed by the Tukey multiple-comparison test was used for statistical comparison of more than two groups. Statistical significance: NS = not significant, and * $p \leq 0.05$.

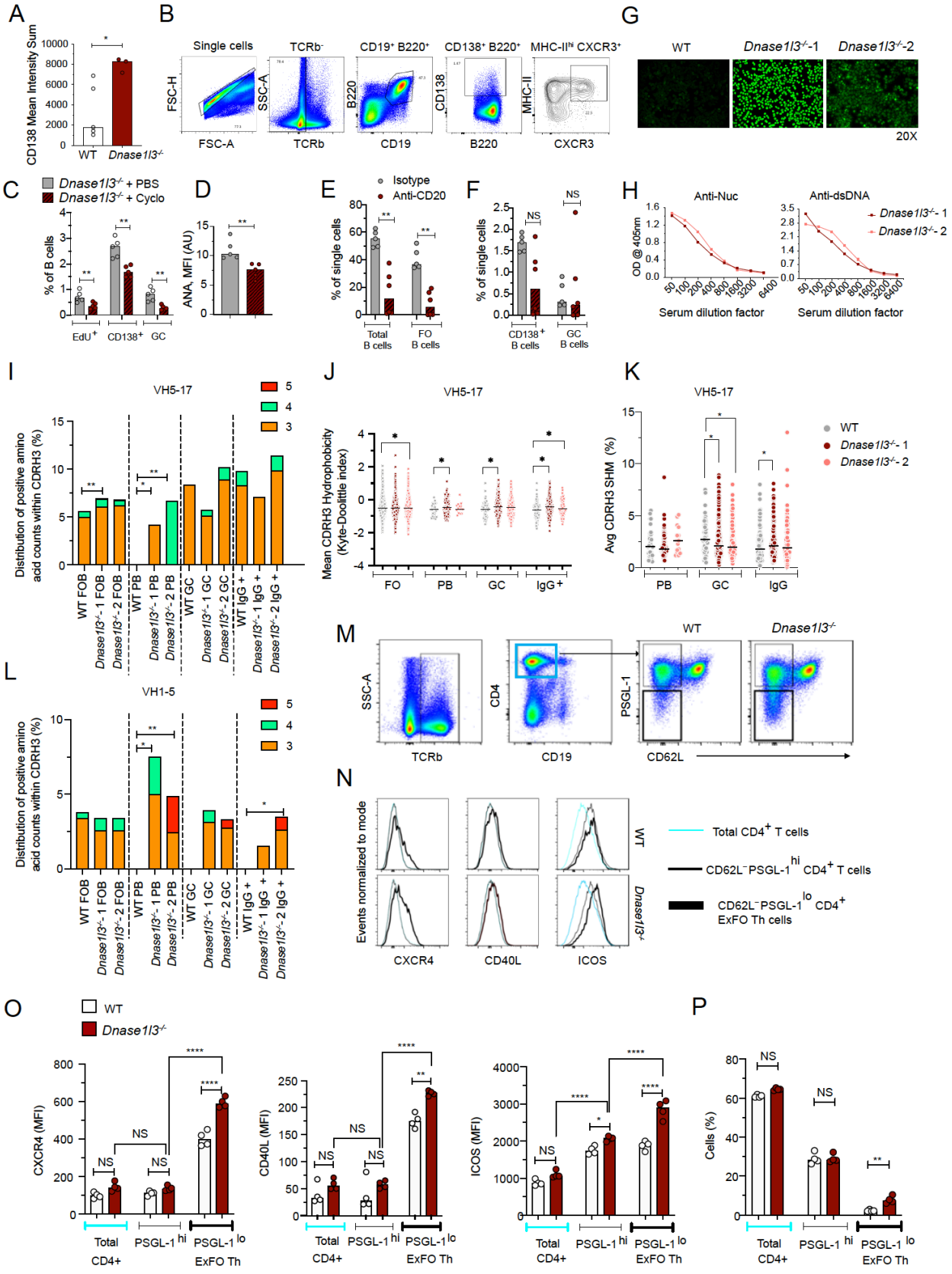

Figure S3. Characteristics of ExFO B cells and ExFO Th cells in WT vs *Dnase1l3*$^{-/-}$mice, Related to Figure 3.

(A) Sum of mean intensity of $CD138^+$ cells in spleen sections of WT (open symbols) vs *Dnase1l3*$^{-/-}$ spleen (red symbols), acquired using confocal microscopy, as in main figure 3, panel A. Symbols represent individual mice and bars indicate median.
(B) Representative flow plots show successive gating strategy used for the characterization of splenic $TCR\beta^-$ $CD19^+B220^{+/low}$ $CD138^{hi}$ cells with high expression of CXCR3 and MHC-II (ExFO B cells) from a *Dnase1l3*$^{-/-}$ mouse.
(C) Frequency of EdU^+ cells, total $CD138^+$ cells and GL-7^+ GC cells among total $B220^+$ $CD19^+$ B cells from the spleens of 6-mo-old *Dnase1l3*$^{-/-}$ mice treated with PBS (grey symbols) or cyclophosphamide (cyclo, red symbols).
(D) ANA fluorescence intensity quantified from HEp-2 slides stained with sera from PBS (grey symbols) or cyclo-treated (red symbols) *Dnase1l3*$^{-/-}$ mice, and probed with secondary anti-Igκ antibody to detect ANAs.
(E, F) Fraction of $TCR\beta^-$ $CD19^+$ total B cells and $TCR\beta^-$ $CD19^+$ $CD23^{hi}$ $CD21^-$ FO B cells (E); $B220^+CD138^+$ Plasmablasts and $B220^+CD38^-$GL-7^+ GC B cells (F), among splenic single lymphocytes in IgG2a isotype (open symbols), and anti-CD20 treated (red symbols) *Dnase1l3*$^{-/-}$ mice at 4 weeks after 2 doses of treatment, as determined by flow cytometry. Significance was estimated using nonparametric Mann-Whitney test.
(G) Fluorescence microscopy images of HEp-2 slides stained with WT or *Dnase1l3*$^{-/-}$-1 or *Dnase1l3*$^{-/-}$-2 mouse sera and probed with secondary anti-Igκ antibody to detect ANAs.
(H) Serum anti-Nucleosome (Nuc,left panel) and anti-dsDNA (right panel), IgG reported as OD at 405nm at the indicated serum dilutions, measured by ELISA.
(I) Percentage of IGHV5-17 clonotypes in each repertoire that contain 3 (yellow), 4 (green), or 5 (red) positively charged amino acids within the CDR-H3 region of indicated B cell subsets and mice.
(J, K) Mean hydrophobicity (Kyte-Doolittle index), and percent distribution of SHM (somatic hypermutation) of the CDR-H3 region among the clonotypes that use V-gene IGHV5-17. Each point represents one clonotype. Error bars represent the mean and S.D. of all clonotypes in each group.
(L) Percentage of IGHV1-5 clonotypes in each repertoire that contain 3, 4, or 5 positively charged amino acids within the CDR-H3 region.
(M) Representative flow plots show gating strategy for the characterization of splenic $CD19^-$ $TCR\beta^+$ $CD4^+$ cells (blue gate) with low levels of PSGL-1 and CD62L (ExFO Th cells, thick black gate) or high-PSGL-1 and low CD62L expression (thin black gate) from WT or *Dnase1l3*$^{-/-}$ mice.
(N, O) Representative histograms show comparative surface expression profile (N) and bar graphs show mean fluorescence intensity (O) of CXCR4, CD40L or ICOS on total $CD4^+$ T cells (blue line), $CD4^+CD62L^-$PSGL-1^{lo} ExFO Th cells (thick black line) and $CD4^+$ $CD62L^-$ PSGL-1^{hi} T cells (thin black line), from splenocytes of 3-mo-old WT (open symbols) and *Dnase1l3*$^{-/-}$ mice (red symbols).
(P) Fraction of $CD4^+$ cells among total splenocytes and PSGL-1^{hi} cells or PSGL-1^{lo} cells among $CD4^+$ T cells from splenocytes of 3-4-mo-old WT (open symbols) or *Dnase1l3*$^{-/-}$mice (red symbols). Symbols represent individual mice and bars indicate median. Significance was estimated using nonparametric Mann-Whitney test. Statistical significance: * $p \leq 0.05$, ** $p \leq 0.01$, and **** $p \leq 0.0001$.

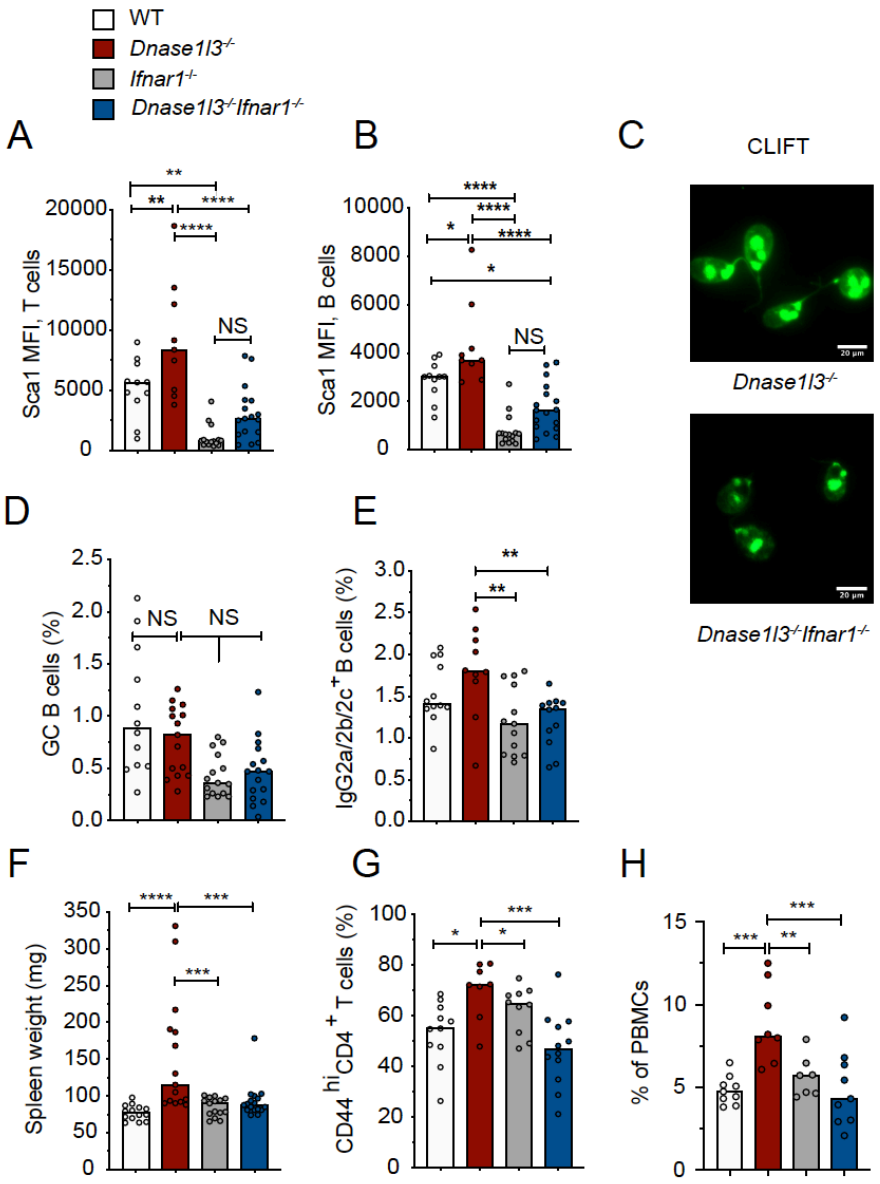

Figure S4. Immune cell activation in *Dnase1l3*$^{-/-}$ mice is governed by type-I IFN signaling, Related to Figure 4.
Dnase1l3$^{-/-}$ (red symbols), *Ifnar1*$^{-/-}$ (grey symbols) were examined along with Dnase1l3/Ifnar1 double-deficient mice (*Dnase1l3*$^{-/-}$*Ifnar1*$^{-/-}$, dark blue symbols) or wild-type controls (WT, open symbols). In panels A-G, symbols represent individual mice and bars indicate median.

(A and B) Mean fluorescence intensity of IFN-inducible antigen Sca-1 on splenic TCRβ^{+}CD4^{+} T cells (A), and CD19^{+}B220^{+} B cells (B), as measured by flow cytometry in the splenocytes of 12-mo-old mice.

(C) Representative images from *Crithidia luciliae* immunofluorescence test (CLIFT). CL substrates were stained with a 1:25 dilution of serum samples from ≥ 4 mice per group. Scale bar: 20μm.

(D and E) Fraction of CD38^{-}GL-7^{+} GC B cells (D) and IgD^{-} IgM^{-} IgG2a/2b^{+} (switched) B cells (E), among CD19^{+} B220^{+} splenic B cells in the splenocytes of 12-mo-old mice, as determined by flow cytometry.

(F) Spleen weight of 12-mo-old mice.

(G) Fraction of CD62L^{-}CD44^{hi} T cells among splenic CD4^{+} T cells in 12-mo-old mice as determined by flow cytometry in the splenocytes of 12-mo-old mice.

(H) Fraction of CD11c^{+} CD11b^{+} Ly6c^{-} population among total PBMCs, in 12-mo-old mice as determined by flow cytometry.

One-way ANOVA followed by the Tukey multiple-comparison test was used for statistical comparison of more than two groups. Statistical significance: NS= not significant, * $p \leq 0.05$, ** $p \leq 0.01$, ***$p \leq 0.001$ and **** $p \leq 0.0001$.

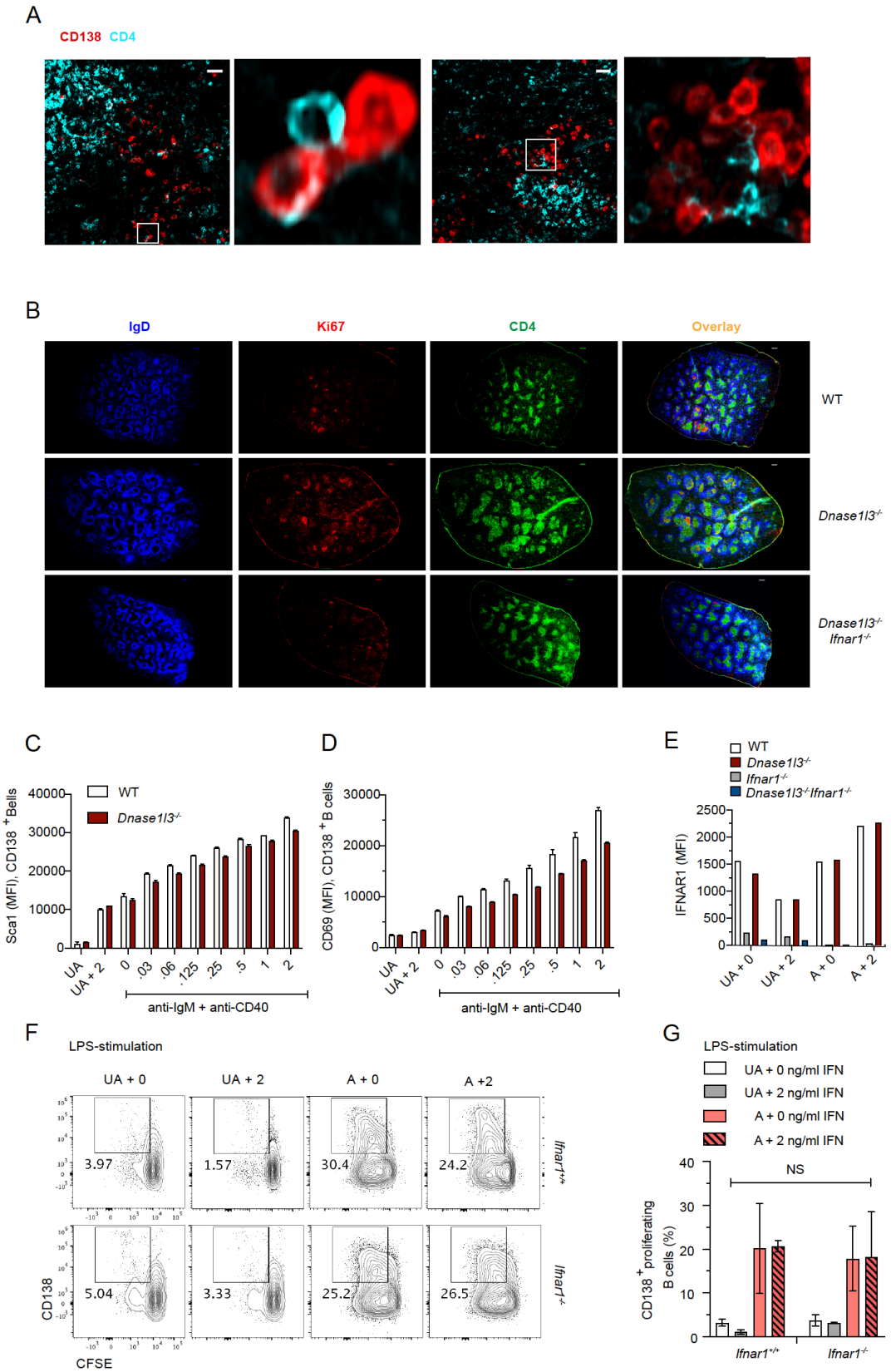

Figure S5. Role of IFNα in the differentiation of B cells into plasmablasts in vitro, Related to Figure 5.

(A) Representative confocal images of spleen sections from three, 8-9-mo-old *Dnase1l3*$^{-/-}$ mice showing the distribution of CD4^{+} T cells near CD138^{+} cell clusters. White insets highlight the close interactions of CD4^{+} T cells with CD138^{+} cells, as shown in magnified images in adjacent panels. Scale bars, 40μm

(B) In situ analysis of proliferating cells in the spleens of WT, *Dnase1l3*$^{-/-}$ and *Dnase1l3*$^{-/-}$*Ifnar1*$^{-/-}$ mice by confocal microscopy. Shown are representative stitched images of spleen sections from at least three >8-mo-old mice of the indicated strains, stained for IgD^{+} naïve follicular B cells (blue), Ki67^{+} proliferating cells (Red), and CD4^{+} T cell zones (green). Right most panels show overlay. Scale bars, 150μm.

(C and D) Analysis of in-vitro activated B cells supplemented with increasing concentration of IFNα. Mean fluorescence intensity of IFN-inducible markers Sca-1 (A) and CD69 (B), on purified B cells from WT (open bars) or *Dnase1l3*$^{-/-}$ (red bars) mice, left unactivated (UA), or cultured with 2 ng/ml IFNα (UA+2) or activated with anti-IgM and anti-CD40 for 72h in the presence increasing concentration of IFNα (0-2 ng/ml), as determined by flow cytometry. Data are representative of two independent experiments with each treatment in duplicate.

(E) Mean fluorescence intensity (MFI) of Ifnar on B cells from WT (open bars), *Ifnar1*$^{-/-}$ (grey bars), *Dnase1l3*$^{-/-}$ (red bars) and *Dnase1l3*$^{-/-}$*Ifnar1*$^{-/-}$ (blue bars) mice, left unactivated (UA) or activated with anti-IgM + anti-CD40 (A) for 72h in the absence (0) or presence of 2 ng/ml of IFNα, measured by flow cytometry. Data are representative of five experiments.

(F) Analysis of proliferation and differentiation of naïve B cells upon in-vitro activation with 1 μg/ml LPS in the presence or absence of IFNα. Shown are representative flow plots of purified CFSE labeled unactivated (UA) or LPS activated (A) B cells from IFNAR-sufficient (*Ifnar1*$^{+/+}$) or IFNAR-deficient (*Ifnar1*$^{-/-}$) mice cultured for 72h in the absence (0 ng/ml) or presence of 2 ng/ml of IFNα. The cells in the gate indicate CFSE^{lo}CD138^{+} proliferating B cells, under the indicated conditions.

(G) Quantification of the percentage of CD138^{+} proliferating *Ifnar1*$^{+/+}$ or *Ifnar1*$^{-/-}$ B cells 72h after in-vitro activation with 1 μg/ml LPS in the presence or absence of IFNα. Error bars show mean $\pm$ SD. Data are representative of two independent experiments. 2-way ANOVA followed by the Tukey multiple-comparison test was used to compare different treatments within a genotype or 2-way ANOVA followed by Sidak's multiple comparison test was used to compare different treatments between the two genotypes. Statistical significance: NS= not significant.

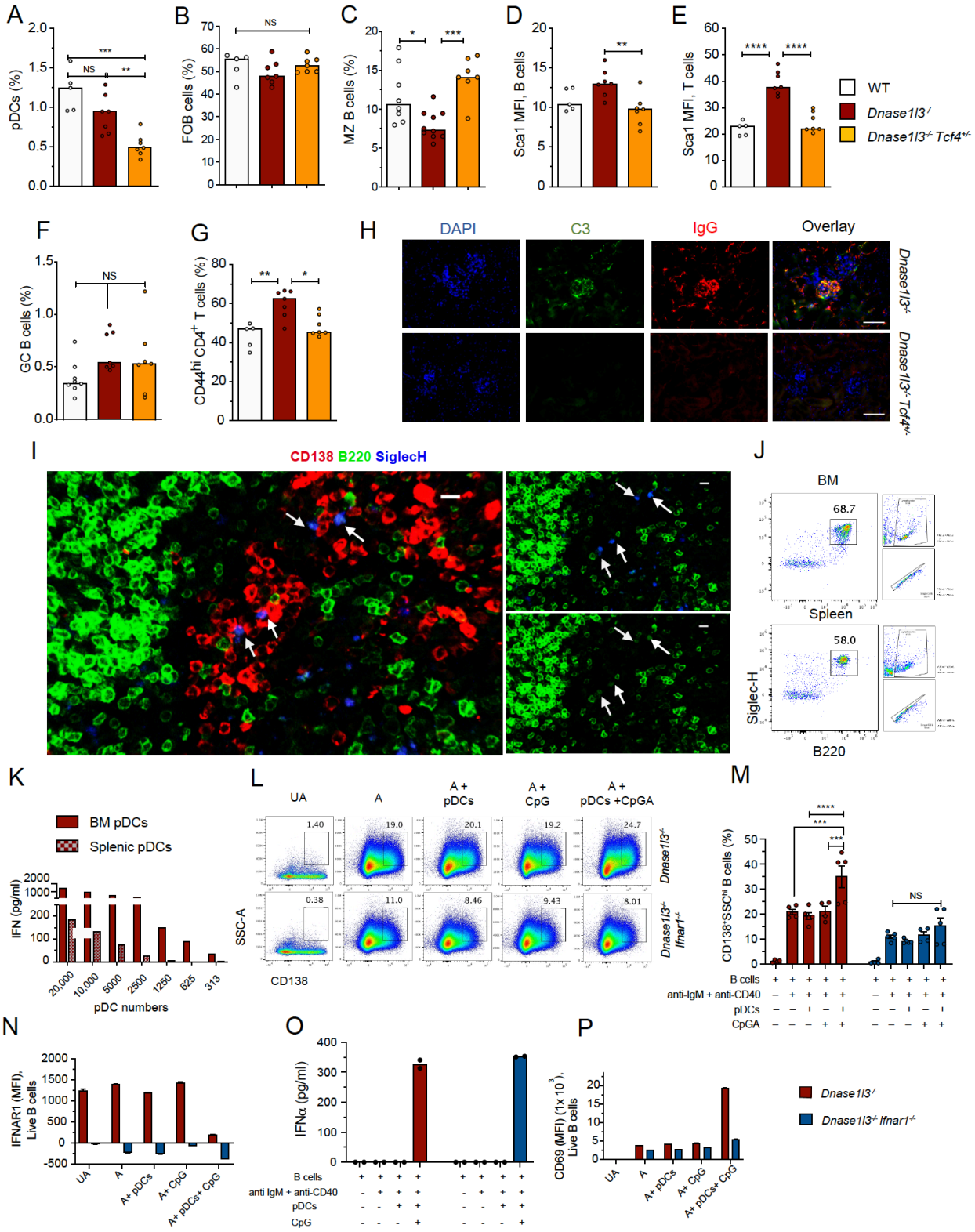

Figure S6. IFNα produced by pDCs promotes differentiation of B cells into plasmablasts, Related to Figure 6.
Dnase1l3$^{-/-}$ (red symbols) were examined along with *Dnase1l3*$^{-/-}$ mice with monoallelic deficiency of TCF4 (*Dnase1l3*$^{-/-}$.*Tcf4*$^{+/-}$, orange symbols) and wild-type controls (WT, open symbols). In panels A- G, symbols represent individual mice and bars indicate median.
(A) Fraction of CD11c^{int}Siglec-H^{+} pDCs among total splenocytes in 12-mo-old mice, determined by flow cytometry.

(B and C) Fraction of TCRβ$^-$CD19$^+$CD23^{hi}CD21$^-$ FO B cells (B) and TCRβ$^-$CD19$^+$ CD23^{lo}CD21^{hi} MZ B cells (C), among splenic single lymphocytes from 12-mo-old mice as determined by flow cytometry.
(D and E) Mean fluorescence intensity of IFN-I inducible antigen Sca-1 on total splenic CD19$^+$B220$^+$ B cells (D) and TCRβ$^+$ T cells (E), as measured by flow cytometry.
(F and G) Fraction of CD38$^-$GL-7$^+$ GC B cells among CD19$^+$B220$^+$ splenic B cells (F), and fraction of CD62L$^-$CD44^{hi} effector T cells among splenic CD4$^+$ T cells (G) in the splenocytes of 12-mo-old mice as determined by flow cytometry. One-way ANOVA followed by the Tukey multiple-comparison test was used for statistical comparison of more than two groups. GraphPad Prism 8 software (La Jolla, CA) was used for all the analyses. Statistical significance: NS= not significant, * $p \leq 0.05$, ** $p \leq 0.01$, *** $p \leq 0.001$ and **** $p \leq 0.0001$.
(H) Representative immunofluorescence images from kidney sections stained for glomerular immune complexes (IgG, red) and C3 (green). Glomeruli identified as nuclei dense (DAPI$^+$, blue) areas in the cortical region of the kidney. Kidneys from at least 3-4, 12-mo-old mice per strain were analyzed. Right most panels show overlay. Scale bars, 50 μm.
(I) In situ analysis of pDCs in the spleens of *Dnase1l3*$^{-/-}$ mice by confocal microscopy. Shown is a representative image of a spleen section from at least three >8-mo-old *Dnase1l3*$^{-/-}$ mice stained for CD138$^+$ plasmablasts (red), B220$^+$(green) and Siglec-H$^+$ (blue) pDCs. Left panel shows the overlay staining with all antibodies while the right side upper and lower panels show B220^{lo} and SiglecH$^+$ pDCs. White arrows indicate the specific pDCs (SiglecH$^+$ B220^{lo}) in close contact with CD138$^+$ plasmablasts in the red pulp. Scale bar, 20 μm.
(J) Assessment of Siglec-H$^+$B220^{lo} pDC purity by flow cytometry after isolation from bone marrow (BM) cells or splenocytes (Spleen) by negative selection using magnetic-activated cell sorting.
(K) Purified BM pDCs (red bars) or splenic pDCs (checkered bars) were cultured at the indicated cell numbers along with 1μM CpGA for 18h and the concentration IFNα secreted in respective culture supernatants were measured by ELISA.
(L-P) Purified CFSE labeled B cells from *Dnase1l3*$^{-/-}$ (red) or *Dnase1l3*$^{-/-}$*Ifnar1*$^{-/-}$ (dark blue) mice: left unactivated (UA); activated with anti-IgM+ anti-CD40 (A); activated with anti-IgM+ anti-CD40 in the presence of unstimulated pDCs (A+ pDCs); Or 1μM CpGA (A+ CpGA) or in the presence of pDCs stimulated with1μM CpGA (A+ pDCs+ CpGA) for 72h.
(L) Representative flow plots show gating strategy for blasting SSC^{hi} B cells positive for CD138.
(M) Quantification of the fraction of CD138$^+$SSC^{hi} blasting B cells.
Error bars show mean ± SD from at least four independent experiments. For statistical analysis of grouped data, two-way ANOVA followed by Tukey's multiple-comparison test was used. Statistical significance: NS= not significant, *** $p \leq 0.001$ and **** $p \leq 0.0001$.
(N) Representative experiment showing mean fluorescence intensity of Ifnar1 on B cells by flow cytometry after the indicated treatments.
(O) Representative experiment showing concentration of IFNα in the culture supernatants of indicated co-cultures as determined by ELISA.
(P) Representative experiment showing mean fluorescence intensity of CD69 on B cells by flow cytometry.

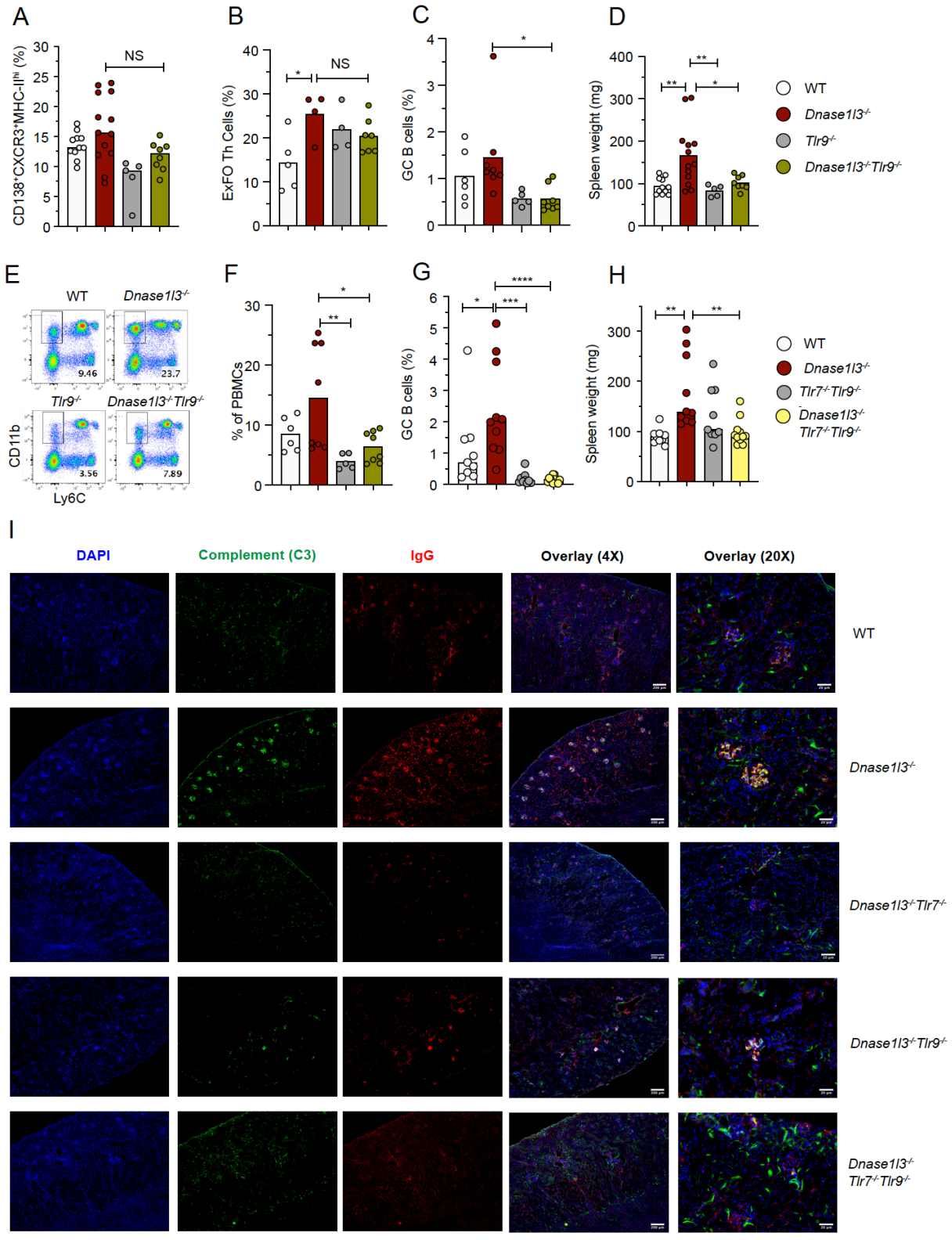

Figure S7. Contribution of TLR9 and TLR7 to autoimmune manifestations of *Dnase1l3*$^{-/-}$ mice, Related to Figure 7.

In panels A-F, 12-mo-old WT control mice (open symbols) *Dnase1l3*$^{-/-}$ (red symbols) were examined along with TLR9-deficient mice (*Tlr9*$^{-/-}$, grey symbols) and *Dnase1l3*$^{-/-}$ mice with TLR9 deficiency (*Dnase1l3*$^{-/-}$*Tlr9*$^{-/-}$, olive-green symbols).

(A) Fraction of CXCR3^{+}MHC-II^{hi} cells among CD138^{+} B cell, as determined by flow cytometry.

(B) Fraction of CD62L^{-}PSGL-1^{lo} cells among CD4^{+} T cells, as determined by flow cytometry.

(C) Fraction of CD38^{-}GL-7^{+} cells among CD19^{+} B cells, as determined by flow cytometry.

(D) Comparative analysis of spleen weights of 12-mo-old mice from the indicated strains.

(E) Representative flow plots of PBMCs from 12-mo-old indicated mice with CD11b^{+}Ly6c^{-} myeloid cells highlighted within the gate.

(F) Fractions of CD11b^{+}Ly6c^{-} population among total PBMCs, as determined by flow cytometry.

(G-H) Fraction of CD38^{-}GL-7^{+} cells among CD19^{+} B cells (G) and comparative analysis of spleen weights (H), of 12-mo-old WT control (open symbols), *Dnase1l3*$^{-/-}$ (red symbols), dual Tlr7 and Tlr9-deficient (*Tlr7*$^{-/-}$*Tlr9*$^{-/-}$, grey symbols) and Dnase1L3, Tlr7 and Tlr9 triple deficient (*Dnase1l3*$^{-/-}$*Tlr7*$^{-/-}$*Tlr9*$^{-/-}$, yellow symbols) mice.

One-way ANOVA followed by the Tukey multiple-comparison test was used for statistical comparison of more than two groups. GraphPad Prism 8 software (La Jolla, CA) was used for all the analyses. Statistical significance: NS= not significant, * $p \leq 0.05$, ** $p \leq 0.01$, *** $p \leq 0.001$ and **** $p \leq 0.0001$.

(I) Representative immunofluorescence images from kidney sections stained for glomerular immune complexes IgG (red), and C3 (green). Glomeruli identified as nuclei dense (DAPI^{+}, blue) areas in the cortical region of the kidney. Kidneys from at least four, 12-mo-old mice per strain were analyzed. Right most panels show overlay at 4X magnification of the cortical region of the kidney (scale bar: 200 μm), and overlay at 20X magnification highlighting individual glomeruli (scale bars, 20μm).